Manuscript type: Full paper

A method for subject-specific modelling and optimisation of the cushioning properties of insole materials used in diabetic footwear

Panagiotis E. Chatzistergos[(1),(*)], Roozbeh Naemi[(1)], Nachiappan Chockalingam[(1)]

(1) CSHER, Faculty of Health Sciences, Staffordshire University, Stoke-on-Trent, United Kingdom.

(*) Corresponding author, **tel.:** +44 1782 295920

e-mail: panagiotis.chatzistergos@staffs.ac.uk, pchatzistergos@gmail.com

Keywords: Finite element, heel- pad, ultrasound indentation, inverse engineering, contact analysis, plantar pressure, plantar soft tissue, diabetic foot, hyperfoam

Abstract:

This study aims to develop a numerical method that can be used to investigate the cushioning properties of different insole materials on a subject-specific basis.

Diabetic footwear and orthotic insoles play an important role for the reduction of plantar pressure in people with diabetes (type-2). Despite that, little information exists about their optimum cushioning properties.

A new in-vivo measurement based computational procedure was developed which entails the generation of 2D subject-specific finite element models of the heel pad based on ultrasound indentation. These models are used to inverse engineer the material properties of the heel pad and simulate the contact between plantar soft tissue and a flat insole. After its validation this modelling procedure was utilised to investigate the importance of plantar soft tissue stiffness, thickness and loading for the correct selection of insole material.

The results indicated that heel pad stiffness and thickness influence plantar pressure but not the optimum insole properties. On the other hand loading appears to significantly influence the optimum insole material properties. These results indicate that parameters that affect the loading of the plantar soft tissues such as body mass or a person's level of physical activity should be carefully considered during insole material selection.

1. Introduction

The diabetic foot disease is one of the most common complications of type-2 diabetes. Previous reports highlight that approximately 15% of people with diabetes world-wide will at some stage develop diabetic foot ulceration that could lead to amputation[1]. The complications of diabetes (type-2) are the most frequent cause of non-traumatic lower-limb amputations[1]. While in the UK up to 100 people/week have a limb amputated as a result of diabetes, it is indicated that up to 80% of these amputations could have been prevented with correct management[2].

Even though it is clear that certain areas of the foot have a significantly higher risk for ulceration (i.e. metatarsal head area, the heel and the hallux)[3] the mechanisms behind ulceration are not yet fully understood. Foot ulcers in people with diabetes are multi-factorial and linked to a variety of clinical risk factors, like peripheral neuropathy and vascular insufficiency[4], as well as biomechanical risk factors, such as increased plantar pressure[3].

Previous in-vivo studies performed with age-matched groups of non-diabetic and diabetic volunteers have found that diabetic plantar soft tissue tends to be thicker[5], stiffer[5,6], harder[7] and to return less energy after a load/unload cycle (i.e. higher energy dissipation ratios)[8]. Moreover recent in-vivo results revealed statistically significant correlations between the stiffness of the heel pad of people with diabetes (type-2) and their blood sugar and triglycerides levels[9].

One of the most common experimental techniques used to study the in-vivo mechanical behaviour of plantar soft tissues is ultrasound indentation. During the indentation test tissue deformation is measured from the ultrasound images[5,8–10] and the applied force is measured from a load sensor enabling the calculation of a force/deformation curve. This curve describes the macroscopic response of the plantar soft tissue to loading and is influenced by the morphology of the tissue as well as by the size and shape of the indenter. The effect of indenter size was numerically investigated by Spears et al.[11] to conclude that larger indenters can produce more reliable and robust measurements compared to smaller ones.

In order to produce a more accurate and objective technique for the material characterisation of plantar soft tissue Erdemir et al.[10] combined the in-vivo indentation test with finite element (FE) modelling. Axisymmetric FE models of the indentation test were used to inverse engineer the values of the material coefficients of a simplified hyperelastic bulk soft tissue.

One of the main therapeutic objectives for the management of the diabetic foot syndrome is the reduction of plantar pressure. Although, therapeutic footwear and orthotic insoles play an important role in redistributing the plantar load[12–15], very little information exists on the optimum cushioning properties of the materials used as foot beds, insoles or a sole. Whilst the criteria for the selection of orthotic insole materials, which were devised some time ago, identify stiffness[16] and the material's "pressure distributing properties"[17] as critical factors for selection, no quantitative method exists to identify the most appropriate material on a subject-specific basis[18,19]. As it stands there is no guideline about how "soft" or "stiff" an insole should be. Despite that, currently there is a huge number of commercially available insole materials and new ones are produced every year.

In this context the purpose of this study is to set the basis for an integrated procedure for the subject-specific FE modelling of the heel pad upon which the investigation of the mechanical compatibility between heel and insole would be possible. Such procedure would allow the optimal cushioning of the insole to be determined based on subject-specific characteristics.

2. Methods

2.1 Ultrasound indentation

A healthy volunteer (age= 38 y, body mass= 82 Kg) was recruited for the purpose of this study. Ethical approval was sought and granted by the University Ethics Committee and the subject provided full informed consent.

An ultrasound indentation device (Figure 1) comprising an ultrasound probe connected in series with a load cell (3kN, INSTRON) was utilised to perform indentation tests at the area of the apex of the calcaneus[9]. The instrumented probe was mounted on a rigid metallic frame that is equipped with a ball-screw linear actuator and a hand-wheel for the manual application of loading as well as with adjustable foot supports to fix the subject's foot (Figure 1). A complete anti-clockwise revolution of the hand wheel generates 5 mm of linear movement in the forward direction. During loading and unloading the crank handle was rotated with a target shaft angular velocity of 90 deg/sec with the help of a metronome. The actual deformation rate that is imposed by the device for this target angular velocity had been previously measured during the pilot testing of the device to be equal to 0.96 mm/sec ± 0.14 mm/sec[9]. This measurement was based on the results of heel indentation tests from 17 healthy subjects[9].

The tests were performed using an 18 MHz linear array ultrasound probe (MyLab25,Esaote,Italy) which is capable of imaging the entire width of the calcaneus. More specifically the footprint area of the ultrasound probe was 3.5 cm^2 and its field-of-view was 42 mm wide and 40 mm deep. Before testing, the subject's right foot was fixed on the device and the instrumented probe was carefully positioned to image the medio-lateral (frontal) plane of the apex of the calcaneus (Figure 2A). The test's imaging plane was identified from sequential ultrasound images of the heel at different planes[9]. During loading the instrumented probe was pressed against the plantar side of the heel compressing the heel pad. More specifically, the heel of the volunteer was subjected to five preconditioning load/unload cycles followed by three measurement cycles to a maximum compressive force of 80 N. The applied force was recorded using the load cell while the initial thickness and the deformation of the heel pad was measured after the completion of the test from the ultrasound images (Figure 1) with the help of video analysis software (Kinovea open source project, www.kinovea.org). Data were sampled at 28 Hz and utilised after the completion of the tests to create an average force/deformation curve. After the completion of the loading procedure and before releasing the subject's foot from its supports the width of the heel was also measured using a digital calliper. The measurement was taken on the ultrasound imaging plane which was identified using the ultrasound probe as a guide. The reproducibility of this simple measurement was established through a test/ re-test procedure.

The magnitude of the applied load (i.e. 80 N) was decided based on preliminary barefoot plantar pressure measurements. More specifically a pressure sensor (F-scan®, Tekscan, Boston, MA, US) was used to measure the peak pressure of the entire heel area during quiet stance and then to calculate the net compressive force that is applied to a section of the heel that is similar to the one imaged during the indentation test. This section was defined around the location of peak pressure and its thickness was the same as the ultrasound probe. Ten trials were performed in total where peak pressure and compressive force were recorded for 15 sec with sampling frequency of 2 Hz. The average peak pressure and compressive force were calculated for each trial.

2.2 Inverse engineering of the material coefficients of heel pad

The inverse engineering of the material coefficients of the plantar soft tissue entails the design of a subject-specific FE model of the indentation test. More specifically the indentation test is simulated using a 2D (plane stress with thickness) FE model comprising a rigid calcaneus and a bulk soft tissue. The geometry of the model is reconstructed from an ultrasound image showing the heel pad under maximum compression (Figure 2A). Using Matlab to outline the calcaneus (Figure 2B) a series of key-points is defined and imported into the FE simulation software (ANSYS 12) to create the FE model of the heel(Figure 2C). The thickness of the soft tissue in the FE model is modified to correspond to the initial tissue thickness measured from the indentation test. The model's width was also uniformly expanded to the value of the measured heel width (Figure 2C). The model of the heel was meshed with 4-node quadrilateral elements (Plane182) using a free-mesh generator[20]. On the other hand the ultrasound probe was simulated as a rigid trapezoid that is in frictionless contact with the plantar side of the soft tissue (Figure 2C). The indentation procedure was simulated by fixing the probe and imposing a displacement to the calcaneus equal to the maximum deformation measured experimentally. This simulation enables the numerical estimation of the force/deformation curve for the indentation test.

The heel pad was simulated as nearly incompressible[21–23] Ogden hyperelastic (1st order) material. The strain energy potential for this material model is defined as follows[20]:

$$W = \frac{\mu_{tissue}}{\alpha_{tissue}}\left(\bar{\lambda}_1^{\ \alpha_{tissue}} + \bar{\lambda}_2^{\ \alpha_{tissue}} + \bar{\lambda}_3^{\ \alpha_{tissue}} - 3\right) + \frac{1}{d_{tissue}}(J-1)^2 \qquad (1)$$

where $\bar{\lambda}_p^{\ a} (p = 1,2,3)$ are the deviatoric principal stretches, J is the determinant of the elastic deformation gradient and μ_{tissue}, α_{tissue} and d_{tissue} are the material coefficients defining the mechanical behaviour of the material. Coefficients μ_{tissue} and α_{tissue} are indirectly related to the material's initial shear modulus and strain hardening/softening respectively while coefficient d_{tissue} is directly related to the material's Poisson's ratio (ν). Assuming that the heel pad is nearly incompressible (i.e. v=0.499) leaves only two material coefficients to be calculated (i.e. μ_{tissue} and α_{tissue}). For this purpose an optimization algorithm was employed to find the values of μ_{tissue} and α_{tissue} that minimize the difference between the numerical and the experimental force/deformation curves. Please also see supplementary material for more information on the inverse engineering procedure (Suppl.Mat.1).

2.3 Simulation of the contact between heel and insole material

The subject-specific model of the indentation test was modified to simulate the contact between the heel pad and an insole material. More specifically the FE model of the rigid ultrasound probe was replaced by a layer of a compliant foam material with uniform thickness of 10 mm (Figure 4A). The friction coefficient between the heel pad and the insole material was set to 0.5[10]. The mechanical behaviour of the foam material was simulated using the Ogden hyperelastic foam model (1st order). The strain energy potential for this material model is defined as follows[20]:

$$W = \frac{\mu_{foam}}{\alpha_{foam}}\left(J^{a_{foam}/3}(\bar{\lambda}_1^{\ a_{foam}} + \bar{\lambda}_2^{\ a_{foam}} + \bar{\lambda}_3^{\ a_{foam}}) - 3\right) + \frac{\mu_{foam}}{a_{foam}\beta_{foam}}(J^{-a_{foam}\beta_{foam}} - 1) \qquad (5)$$

where $\bar{\lambda}_p^{\ a_{foam}} (p = 1,2,3)$ are the deviatoric principal stretches, J is the determinant of the elastic deformation gradient and μ_{foam}, α_{foam} and β_{foam} are the material coefficients. Coefficients μ_{foam} and

α_{foam} are indirectly related to the material's initial shear modulus and strain hardening/softening respectively while β_{foam} is directly related to the material's Poisson's ratio (ν).

The material coefficients of the foam material were initially assigned for commercially available PU foam that is used in diabetic footwear. These values were not available from the manufacturer and were calculated following a combined experimental and numerical approach as follows: μ_{PU} =39.6 kPa, α_{PU}=19.3, ν_{PU}= 0.06 (please also see supplementary material (Suppl.Mat.2)).

The aforementioned modelling procedure for the contact between the heel and an insole material was used to give an insight in the optimum cushioning properties of flat insoles. The numerical calculations performed to quantify the cushioning properties of an insole material were: the maximum deformation of the insole material under constant load, the energy that is absorbed during loading, the peak plantar pressure and the percent reduction of peak plantar pressure. Pressure reduction was calculated relatively to barefoot standing on a rigid surface which was simulated by multiplying the μ_{foam} material coefficient of the PU foam by 10^6 to turn the simulated insole material into a practically rigid body. Quiet stance was simulated by fixing the lower surface of the foam layer and applying a net compressive force of 80N at the calcaneus.

2.4 Validation

The accuracy of the predicted peak pressures between the heel pad and the insole material was assessed through a testing procedure that closely matched the numerically simulated loading scenario (Figure 5). For this purpose the ultrasound probe of the previously described ultrasound indentation device was replaced with a rigid support for insole materials and the foot was loaded through a rectangular cuboid (120 mm ×10 mm ×10 mm) piece of the previously mentioned PU foam. A thin plantar pressure sensor (F-scan®, Tekscan, Boston, MA, US) was also placed between the foot and the foam to measure peak pressure. The subject's foot was subjected to five preconditioning load/unload cycles and three measuring ones to a maximum compressive force of 80 N. During the last three load cycles the imposed force and the peak plantar pressure between the foot and the PU foam were recorded at 28Hz. Both the loading rate and the sampling rate used for this test were identical to those of the indentation tests. At the end the peak pressure developed for 80 N of applied compression was averaged for the three trials and then compared with the numerically calculated one.

An additional series of in-vivo measurements was performed to validate the ability of the subject-specific FE model to predict the peak pressure reduction that is achieved by a foam material. For this purpose plantar pressure measurements were performed with the subject standing (barefoot) on a 10 mm thick sheet of the PU foam. Ten trials were performed in total and for each one of them the peak pressure of the entire heel area was recorded for 15 sec. Considering the non-dynamic nature of loading a relatively low sampling rate (2 Hz) was considered to adequately capture the plantar pressure during quiet stance. After averaging, these results were compared to the ones recorded for the subject standing barefoot on a rigid surface to calculate the percent pressure reduction achieved by the PU foam. At the end the experimentally measured pressure reduction was compared to the numerically calculated one.

2.5 Parametric analyses

The aim of the first parametric investigation was to assess the sensitivity of the insole's cushioning properties to its material coefficients μ_{foam} and α_{foam}. For this purpose 72 scenarios were simulated in total for twelve different values of μ_{foam} ranging between 10 k Pa $\leq \mu_{foam} \leq$ 210 kPa (i.e. increments of 21 kPa) and six values of α_{foam} between $2 \leq \alpha_{foam} \leq 12$ (i.e. increments of 2). The Poisson's ratio of the foam material was kept constant ($\nu_{foam} = \nu_{PU}$).

The second parametric investigation aimed to assess the importance of subject-specific heel pad material properties for the correct selection of insole material. Three scenarios were included in this investigation for the cases of "average stiffness", "soft" and "stiff" heel pads. The case of "average stiffness" was simulated using the material coefficients that were inverse engineered from the ultrasound indentation tests. The remaining two cases were reconstructed based on literature by decreasing the values of the tissue's material coefficients μ_{tissue} and α_{tissue} (Equation 1) by 50% or increasing them by 50% respectively to simulate a "softer" or "stiffer" heel pad respectively[10].

The aim of the third parametric investigation was to assess the importance of subject-specific tissue thickness for the correct selection of insole material. Three scenarios were included in this investigation, namely for a heel pad of "average thickness" as well as for "thin" and "thick" heel pads. The last two cases were simulated by decreasing or increasing the thickness of the heel pad respectively by 50%[5,10].

The aim of the last parametric investigation was to assess the importance of loading for defining the optimum cushioning properties of insole materials. For this purpose the net force applied to the FE model was increased from 80N to 160 N and 240 N (100% and 200% increase).

For each one of the aforementioned analyses the pressure reduction that can be achieved by foam materials that exhibit different mechanical behaviour was assessed. The mechanical behaviour of the foam was modified by changing the value of μ_{foam} ($10\ \text{kPa} \leq \mu_{foam} \leq 200\ \text{kPa}$) while α_{foam} and ν_{foam} (Equation 5) were kept constant. Initially coefficient α_{foam} was set equal to the optimum value found during the first parametric investigation while ν_{foam} was equal to ν_{PU}. One higher and one lower value of α_{foam} were also included in the investigation (increments of 2).

3. Results

3.1 Ultrasound indentation

The preliminary plantar pressure measurements showed that the average(±stdev) peak pressure for all ten trials of barefoot standing on a rigid surface was equal to 176 kPa (±7.6 kPa) while the average(±stdev) net compressive force applied to a section of the heel that is similar to the one imaged during the indentation test was 80N (±4N).

The main output of the indentation test was the average force/deformation curve of the heel pad (Figure 3). The reconstructed outline of the calcaneus is shown in figure 2C while the thickness of the heel pad and the width of the heel were measured to be 20.1 mm and 68 mm respectively.

3.2 Inverse engineering of the material coefficients of heel pad

The optimum solution for the inverse engineering procedure (Figure 3) was as follows:

μ_{tissue}= 1.18 kPa and α_{tissue}= 17.38.

3.3 Simulation of the contact between heel and insole material

The numerically estimated peak plantar pressure between the heel pad and the PU foam was 177 kPa (Figure 4C). The maximum deformation of the insole and the work that was absorbed during loading was 51.3% and 0.182 Nm respectively. The respective peak pressure for the case of barefoot standing on a rigid surface was 226 kPa (Figure 4B) which means that the predicted pressure reduction for the PU foam is 21.8%.

3.4 Validation

The average(±stdev) peak pressure that was measured for a testing procedure that closely matched the simulations was 184 kPa (±3kPa). The difference between the experimentally measured peak pressure and the numerically estimated one was 3.8%.

The average(±stdev) peak pressure measured at the heel for barefoot standing on a 10 mm thick sheet of PU foam was 137 kPa (±10 kPa). Considering the value of the peak pressure for barefoot standing on a rigid surface this measurement translates to 22.4 % peak pressure reduction compared to 21.8% that was predicted from the FE analysis.

3.5 Parametric analyses

The sweep of the design space indicated that clear optimum values exist for the insole material coefficients. Peak pressure was minimised for μ_{foam} =52 kPa and α_{foam} =6 and its minimum value was 166 kPa, which corresponds to 26.5% reduction relatively to barefoot standing on a rigid surface (Figure 6A). On the other hand the energy absorbed during loading was maximised for μ_{foam} =31 kPa and α_{foam} =6 (Figure 6B). The maximum value of the absorbed energy during loading was 0.22 Nm. In contrast to peak pressure and absorbed energy the maximum deformation appears to increase with decreasing μ_{foam} and α_{foam} for the entire range of values that were tested (Figure 6C).

Reducing the values of the plantar soft tissue's material coefficients by 50% to produce a "softer" heel pad caused a significant increase of barefoot peak pressure by 19%. On the contrary increasing the values of the coefficients by 50% to simulate a "stiffer" heel pad caused a marginal increase of peak pressure by only 1%.

The maximum pressure reduction achieved for the case of a "softer" or "stiffer" heel pad was 28.4% and 32.4% respectively. In both cases maximum pressure reduction was achieved for α_{foam} =6 (Table 1). As it can be seen in Figure 7A the insole material coefficients (μ_{foam}) that maximise pressure reduction for a "soft" or a "stiff" heel pad appear to be the same as the ones found for a heel pad of "average stiffness". Similarly, altered soft tissue properties appear to have no effect on the insole properties that maximise energy absorption during loading (Figure 7B).

Changing the thickness of the heel pad had a significant effect on barefoot peak pressure. More specifically decreasing heel pad thickness by 50% caused a 25% increase of peak pressure while increasing heel pad thickness by 50% caused a 12% decrease of pressure.

Despite its effect on plantar pressure, heel pad thickness appeared to cause no change to the optimum insole properties. The maximum pressure reduction that was found for the case of a "thin" or "thick" heel pad was equal to 33.8% and 23.1% respectively. In both cases maximum reduction was again achieved for α_{foam} =6 (Table 1). As it can be seen in figures 7C and 7D the value of μ_{foam} that maximises pressure reduction and energy absorbed for the cases of "thin" and "thick" heel pad appears to be the same as for a heel of "average thickness".

Increasing the net compressive force by 100% and 200% increased barefoot peak pressure by 105.7% and 227.6% respectively. In the case of 160 N (i.e. 100% force increase) a maximum pressure reduction of 26.1% was achieved for μ_{foam} = 116 kPa and α_{foam} =6 (Figure 7E). The maximum pressure reduction in the case of 240 N (i.e. 200% force increase) was 29.3% and it was achieved for μ_{foam} = 150 kPa and α_{foam} =6 (Figure 7E). Moreover the maximum value of energy absorbed during loading (Figure 7F) for the cases of 160 N and 240 N was 0.45 Nm and 0.68 Nm for μ_{foam} = 73 kPa and μ_{foam} = 100 kPa respectively (α_{foam} =6).

4. Discussion

Even though current literature is rich with elaborate geometrically detailed FE models of the entire foot[21,22,24,25] and of the heel[26], the design and use of these models is labour intensive, computationally expensive and requires a significant amount of information in terms of tissue geometry and mechanical properties. This makes the extensive use of geometrically detailed FE models impractical for clinical applications or the optimisation of footwear design. The use of anatomically focused simplified models has been proposed as an alternative simulation approach to overcome the aforementioned problems associated with geometrically detailed FE models[23,27].

In this context, the methodology presented here entails the creation of subject-specific 2D FE models of a critical area of the heel based on relatively simple, non-invasive tests, namely ultrasound indentation and plantar pressure measurements. The ultrasound indentation test provides the necessary information for the design of the models and also for the inverse engineering of the material properties of the heel pad.

In a previous study, Erdemir et al.[10] also combined indentation tests with FE modelling to inverse engineer the heel pad's hyperelastic coefficients and reported the average initial shear modulus (K_0) of the heel pads for twenty non-diabetic subjects to be equal to 16.54 kPa with a standard deviation of 8.27[10]. Similarly, the initial shear modulus of the heel pad of the non-diabetic subject of the present study can be calculated as follows: $K_0 = \frac{1}{2}\mu_{tissue}\alpha_{tissue} = 10.25\ kPa$[20]. This value falls well within the range of values reported by Erdemir et al.[10].

This modelling procedure was also employed for the simulation of the contact between the heel and insole materials. As far as peak plantar pressure is concerned, the comparison between numerical and experimental results for a single subject showed that the proposed technique can accurately predict the peak plantar pressure for a loading scenario that closely matches the simulation, namely loading the heel using a strip of foam material (Figure 5). Even though this loading is the closest one can get to the FE simulation, these two loading scenarios are still not identical, mainly because of the shear stresses that are developed between the loaded and unloaded tissues in the case of the in-vivo loading.

This first validation indicates that the proposed simulation technique can correctly solve the simplified problem for which it was designed. Moreover comparing the results for the aforementioned idealised loading scenario and quiet stance showed that the FE simulation overestimates the magnitude of peak pressure but accurately estimates the normalised pressure reduction. More specifically the numerically estimated peak pressure for the idealised loading scenario was 29.2 % higher than the one measured for quiet stance. On the contrary the difference between the predicted and the measured pressure reduction was only 3.0 %.

All pressure measurements were performed using very thin (thickness≈0.25mm) sensors (F-scan®, Tekscan, Boston, MA, US) that cannot offer any cushioning themselves and follow the curvature of the insole. Based on that, the sensor's effect on the results was considered to be negligible and was not included into the FE analysis.

After validation, the subject-specific model was utilised to assess the cushioning properties of different foam materials. The results indicated that correct selection or fine-tuning of the mechanical behaviour of insole materials can maximise an insole's capacity to reduce pressure and absorb energy during loading. Moreover maximising the insole's capacity to reduce plantar pressure does not mean that its capacity to absorb energy during loading is maximised too. Indeed it is indicated that an insole that is slightly "softer" than the one that maximises pressure reduction is needed to maximise energy absorbed (Figure 6).

Previous in-vivo studies have found that the mechanical behaviour[5–8] and the thickness[5] of the plantar soft tissue of people with diabetes change during the course of the disease. The importance of these alterations for the assessment of ulceration risk has been highlighted by a series of numerical analyses which indicate that these changes in mechanical properties and thickness of plantar soft tissues can lead to increased plantar pressures[10,28,29]. Even though it is clear that people that have different risk for ulceration are likely to need different types of footwear the exact implications of altered tissue mechanical properties and thickness for the selection of insole material are not clear. In other words currently no guidelines exist to inform health care professionals working on the diabetic foot if people with different plantar soft tissues stiffness or thickness also need insoles made from different materials. The importance of the correct selection of insole material has been previously highlighted by numerical studies indicating that the pressure-relieving capabilities of footwear[15,30] as well as perceived comfort[25] are significantly influenced by the mechanical properties of the insole material.

In this context the results of this study indicated that even though heel pad mechanical properties and thickness influence plantar pressure they do not affect the optimum cushioning properties of insole materials. Indeed as it can be seen in figures 7A-D the insole material properties that maximise pressure reduction and energy absorbed during loading remain the same regardless of changes in terms of tissue stiffness or thickness. Therefore it can be concluded that these two parameters are not likely to be critical to inform insole material selection. In contrast to subject-specific tissue stiffness and thickness, subject-specific loading appears to significantly influence the optimum insole material properties (Figures 7E,F).

Considering the plantar area of the FE model of the heel pad the three load magnitudes (i.e. 80 N, 160 N, 240 N) that were included in the study correspond to average pressures of 147 kPa, 294 kPa and 441 kPa respectively. These values might be relatively high for static loading scenarios and more likely to be developed during dynamic ones such as walking[31] or running[32], but the simulation revealed a clear trend, indicating that the optimum stiffness of an insole material increased with loading. Even though more testing is needed to confirm these results for dynamic loading the findings of this study indicate that the cushioning properties of insole materials could possibly be optimised on a subject-specific basis using simple information on loading and the factors that influence it (e.g. body mass, a person's type of weight-bearing physical activity etc.).

Moreover further tests involving people with diabetes are also needed to see if a material selection method that is based on loading could also be used to inform the prescription of diabetic footwear. At this point it should be stressed out that the correct selection of materials is only one aspect of footwear that could be optimised on a patient-specific basis. The overall structure of the footwear[33–35] as well as the degree of congruity between the footwear and the foot[28] need also to be considered to maximise the efficiency of diabetic footwear.

Because of the manual operation of the indentation device and limitations in the achievable loading rates the modelling procedure presented here was limited to quasi-static loading scenarios and therefore the viscosity of the plantar soft tissue was not taken into account. Besides that, it is clear from literature that the viscosity can significantly alter the plantar soft tissue's response to dynamic loading and therefore it should be considered in the case of dynamic loading[26,34,36–38].

Another limitation of this modelling procedure is that the use of a 2D model restricts its application to loading scenarios that don't involve considerable out of plane loads. As a result of that the effect of plantar shear stresses, which according to literature are altered in diabetic neuropathic patients and play an important role for ulceration[39,40], cannot be investigated with the existing 2D FE models. On the other hand, the use of a 2D model substantially reduced the computational power that is needed to perform each analysis and enabled its use for the inverse engineering of the heel pad's material coefficients, which is a highly iterative process. In addition, the use of a 2D model significantly simplified the reconstruction of the heel pad's geometry and enabled the design of subject-specific models without the need for CT or MRI scans which are costly and their analysis is very labour intensive. At this point it should be stressed out that the geometry of the calcaneus is expected to influence the results of the analysis and reconstructing it for every subject significantly enhances the subject-specificity of the analysis.

Moreover the assumption that the plantar soft tissue is a uniform bulk material means that this model cannot be used to study the internal stress and strain fields of the tissue. The simplified simulation of the tissue's internal structure could also compromise the reliability of the model for loading cases other than the ones for which it was validated.

On the other hand the proposed modelling procedure was proven to be satisfactory accurate for the simulation of heel pad’s macroscopic response to quasi static loading and the analysis of the contact conditions between the heel pad and different insole materials. This ability enabled a thorough investigation of some important parameters that could affect the mechanical compatibility between the heel pad and insole materials and shed new light on the optimum cushioning properties of insoles without the limitations of commercially available materials. Moreover, the FE modelling procedure presented here offers an improved approach for the inverse engineering of the heel pad’s hyperelastic coefficients[10] which takes into account the subject specific geometry of the calcaneus. In the future the method presented here could also be used for other areas of the foot such as the metatarsal heads or the Hallux.

Competing interests: None declared

Funding: This work is supported through the project titled DiabSmart funded by the European Commission (Grant Agreement Number 285985, Industry Academia partnerships and Pathways (FP7-PEOPLE-2011-IAPP)).

Ethical approval: Ethical approval was sought and granted by the Staffordshire University Ethics Committee.

References

[1] Boulton a J. The diabetic foot: a global view. Diabetes Metab Res Rev 2000;16 Suppl 1:S2–5.

[2] Diabetes UK. Diabetes in the UK 2011– 12 Key Statistics on diabetes. 2011.

[3] Ledoux WR, Shofer JB, Cowley MS, Ahroni JH, Cohen V, Boyko EJ. Diabetic foot ulcer incidence in relation to plantar pressure magnitude and measurement location. J Diabetes Complications 2013;27:621–6.

[4] Crawford F, Inkster M, Kleijnen J, Fahey T. Predicting foot ulcers in patients with diabetes: a systematic review and meta-analysis. QJM 2007;100:65–86.

[5] Chao CYL, Zheng Y-P, Cheing GL-Y. Epidermal thickness and biomechanical properties of plantar tissues in diabetic foot.pdf. Ultrasound Med Biol 2011;37:1029–38.

[6] Klaesner JW, Hastings MK, Zou D, Lewis C, Mueller MJ. Plantar tissue stiffness in patients with diabetes mellitus and peripheral neuropathy. Arch Phys Med Rehabil 2002;83:1796–801.

[7] Piaggesi A, Romanelli M, Schipani E, Campi F, Magliaro A, Baccetti F, et al. Hardness of Plantar Skin in Diabetic Neuropathic Feet. J Diabetes Complications 1999;13:129–34.

[8] Hsu TC, Wang CL, Shau YW, Tang FT, Li KL, Chen CY. Altered heel-pad mechanical properties in patients with Type 2 diabetes mellitus. Diabet Med 2000;17:854–9.

[9] Chatzistergos PE, Naemi R, Sundar L, Ramachandran A, Chockalingam N. The relationship between the mechanical properties of heel-pad and common clinical measures associated with foot ulcers in patients with diabetes. J Diabetes Complications 2014:(in – press).

[10] Erdemir A, Viveiros ML, Ulbrecht JS, Cavanagh PR. An inverse finite-element model of heel-pad indentation. J Biomech 2006;39:1279–86.

[11] Spears IR, Miller-Young JE. The effect of heel-pad thickness and loading protocol on measured heel-pad stiffness and a standardized protocol for inter-subject comparability. Clin Biomech (Bristol, Avon) 2006;21:204–12.

[12] Reiber GE. Who is at risk of limb loss and what to do about it? J Rehabil Res Dev 1994;31:357–62.

[13] Ragnarson Tennvall G, Apelqvist J. Prevention of diabetes-related foot ulcers and amputations: a cost-utility analysis based on Markov model simulations. Diabetologia 2001;44:2077–87.

[14] Healy A, Naemi R, Chockalingam N. The effectiveness of footwear as an intervention to prevent or to reduce biomechanical risk factors associated with diabetic foot ulceration: A systematic review. J Diabetes Complications 2013;27:391–400.

[15] Cheung JT-M, Zhang M. Parametric design of pressure-relieving foot orthosis using statistics-based finite element method. Med Eng Phys 2008;30:269–77.

[16] Shurr D., Cook TM. Methods, materials, and mechanics. Prosthetics Orthot., Prentice Hall; 1990, p. 17–29.

[17] Campbell GJ, McLure M, Newell EN. Compressive behavior after simulated service conditions of some foamed materials intended as orthotic shoe insoles. J Rehabil Res Dev 1984;21:57–65.

[18] Healy A, Dunning DN, Chockalingam N. Materials used for footwear orthoses: a review. Footwear Sci 2010;2:93–110.

[19] Paton JS, Stenhouse E, Bruce G, Jones R. A longitudinal investigation into the functional and physical durability of insoles used for the preventive management of neuropathic diabetic feet. J Am Podiatr Med Assoc n.d.;104:50–7.

[20] ANSYS. ANSYS Release 12 Documentation. Canonsburg, PA, USA: ANSYS Inc; n.d.

[21] Guiotto A, Sawacha Z, Guarneri G, Avogaro A, Cobelli C. 3D finite element model of the diabetic neuropathic foot: A gait analysis driven approach. J Biomech 2014:1–8.

[22] Isvilanonda V, Dengler E, Iaquinto JM, Sangeorzan BJ, Ledoux WR. Finite element analysis of the foot: model validation and comparison between two common treatments of the clawed hallux deformity. Clin Biomech (Bristol, Avon) 2012;27:837–44.

[23] Spirka T a., Erdemir A, Ewers Spaulding S, Yamane A, Telfer S, Cavanagh PR. Simple finite element models for use in the design of therapeutic footwear. J Biomech 2014.

[24] Chen W-M, Lee T, Lee PV-S, Lee JW, Lee S-J. Effects of internal stress concentrations in plantar soft-tissue--A preliminary three-dimensional finite element analysis. Med Eng Phys 2010;32:324–31.

[25] Franciosa P, Gerbino S, Lanzotti A, Silvestri L. Improving comfort of shoe sole through experiments based on CAD-FEM modeling. Med Eng Phys 2013;35:36–46.

[26] Fontanella CG, Wilhjelm JE, Virga a., Carniel EL, Matteoli S, Corvi a., et al. Investigation on the load-displacement curves of a human healthy heel pad: In vivo compression data compared to numerical results. Med Eng Phys 2012;34:1253–9.

[27] Yarnitzky G, Yizhar Z, Gefen A. Real-time subject-specific monitoring of internal deformations and stresses in the soft tissues of the foot: A new approach in gait analysis. J Biomech 2006;39:2673–89.

[28] Goske S, Erdemir A, Petre MT, Budhabhatti S, Cavanagh PR. Reduction of plantar heel pressures: Insole design using finite element analysis. J Biomech 2006;39:2363–70.

[29] Gefen A. Plantar soft tissue loading under the medial metatarsals in the standing diabetic foot. Med Eng Phys 2003;25:491–9.

[30] Luo G, Houston VL, Garbarini MA, Beattie AC, Thongpop C. Finite element analysis of heel pad with insoles. J Biomech 2011;44:1559–65.

[31] Sacco ICN, Hamamoto AN, Tonicelli LMG, Watari R, Ortega NRS, Sartor CD. Abnormalities of plantar pressure distribution in early, intermediate, and late stages of diabetic neuropathy. Gait Posture 2014;40:570–4.

[32] García-Pérez J a, Pérez-Soriano P, Llana S, Martínez-Nova A, Sánchez-Zuriaga D. Effect of overground vs treadmill running on plantar pressure: influence of fatigue. Gait Posture 2013;38:929–33.

[33] Verdejo R, Mills NJ. Heel-shoe interactions and the durability of EVA foam running-shoe midsoles. J Biomech 2004;37:1379–86.

[34] Fontanella CG, Forestiero a, Carniel EL, Natali a N. Analysis of heel pad tissues mechanics at the heel strike in bare and shod conditions. Med Eng Phys 2013;35:441–7.

[35] Cho J-R, Park S-B, Ryu S-H, Kim S-H, Lee S-B. Landing impact analysis of sports shoes using 3-D coupled foot-shoe finite element model. J Mech Sci Technol 2009;23:2583–91.

[36] Pai S, Ledoux WR. The quasi-linear viscoelastic properties of diabetic and non-diabetic plantar soft tissue. Ann Biomed Eng 2011;39:1517–27.

[37] Natali a. N, Fontanella CG, Carniel EL, Young JM. Biomechanical behaviour of heel pad tissue experimental testing, constitutive formulation, and numerical modelling. Proc Inst Mech Eng Part H J Eng Med 2011;225:449–59.

[38] Natali a N, Fontanella CG, Carniel EL. Constitutive formulation and analysis of heel pad tissues mechanics. Med Eng Phys 2010;32:516–22.

[39] Uccioli L, Caselli A, Giacomozzi C, Macellari V, Giurato L, Lardieri L, et al. Pattern of abnormal tangential forces in the diabetic neuropathic foot. Clin Biomech 2001;16:446–54.

[40] Yavuz M, Tajaddini A, Botek G, Davis BL. Temporal characteristics of plantar shear distribution: relevance to diabetic patients. J Biomech 2008;41:556–9.

Tables:

Table 1: The maximum pressure reduction that was achieved for insole materials with α_{foam} = 4, 6 and 8 and for the cases of altered heel pad stiffness, thickness and loading. The respective optimum values of μ_{foam} are also shown in brackets for each one of these cases.

		Heel pad stiffness			**Heel pad thickness**			**Heel pad loading**		
		"Stiff"	**Average**	**"Soft"**	**"Thick"**	**Average**	**"Thin"**	**240N**	**160N**	**80N**
$\alpha_{foam}=4$	**Max. pressure reduction (%)**	31.6 *(52kPa)*	26.4 *(52kPa)*	27.9 *(73kPa)*	22.8 *(52kPa)*	26.4 *(21kPa)*	33.6 *(52kPa)*	29.2 *(150kPa)*	26.3 *(116kPa)*	26.4 *(52kPa)*
$\alpha_{foam}=6$	**Max. pressure reduction (%)**	32.4 *(52kPa)*	26.5 *(52kPa)*	28.4 *(52kPa)*	23.1 *(52kPa)*	26.5 *(52kPa)*	33.8 *(52kPa)*	29.3 *(150kPa)*	26.1 *(116kPa)*	26.5 *(52kPa)*
$\alpha_{foam}=8$	**Max. pressure reduction (%)**	31.8 *(61kPa)*	26.0 *(52kPa)*	27.5 *(61kPa)*	22.5 *(52kPa)*	26.0 *(52kPa)*	32.9 *(52kPa)*	29.1 *(150kPa)*	26.0 *(116kPa)*	26.0 *(52kPa)*

<u>Figure legends</u>

Figure 1: The ultrasound indentation device and a schematic representation of the procedure followed to create the tissue's force/deformation curve.

Figure 2: (A) The frontal ultrasound image of the heel that was used for the reconstruction of the geometry of the calcaneus. (B) Using Matlab the ultrasound image is divided by a series of line segments with a relative distance of 2 mm. These lines are used as "search paths" to identify the transition points between bone and soft tissue. When imported into ANSYS the coordinates of these key points are utilised to create a polynomial line that outlines the calcaneus. (C) The geometry of the final FE model of the indentation test.

Figure 3: The experimental force/deformation curve for the indentation test and the respective numerical curve for the final best solution for the inverse engineering procedure.

Figure 4: (A) The FE model that was used for the estimation of plantar pressure and its application for the cases of barefoot standing on a rigid surface (B) and barefoot standing on a 10mm thick sheet of an insole material (C). The material properties of this insole material correspond to the PU foam used for the validation of the model. Both pressure distributions (Pa) are calculated for a maximum load of 80N and their peak values were used to calculate the pressure reduction that can be achieved by the PU foam.

Figure 5: A schematic representation of a loading scenario that closely matches the performed simulations and was used for the validation of the subject-specific FE model.

Figure 6: The reduction of peak plantar pressure (A), the total energy absorbed during loading (B) and the maximum deformation of the insole material (C) for insoles that have different mechanical behaviour as defined by different μ_{foam} and α_{foam} values. The peak values of each graph are marked with star.

Figure 7: The effect of different heel pad stiffness (A, B), thickness (C,D) and loading (E,F) to the optimum cushioning properties of an insole material. For each one of these cases the reduction of peak plantar pressure (%) and the total energy absorbed during loading (Nm) is presented for insoles that have different stiffness. To improve clarity, the results presented in this figure correspond to insole materials that have different μ_{foam} coefficients but the same α_{foam} coefficient (i.e. $\alpha_{foam} = 6$).

Supplementary material captions

Suppl. Mat. 1: A detailed description of the method that was used to inverse engineer the material coefficients of the heel-pad.

Suppl. Mat. 2: The methodological approach for the calculation of the hyperelastic material coefficients of commercially available PU foam.

Figure 1

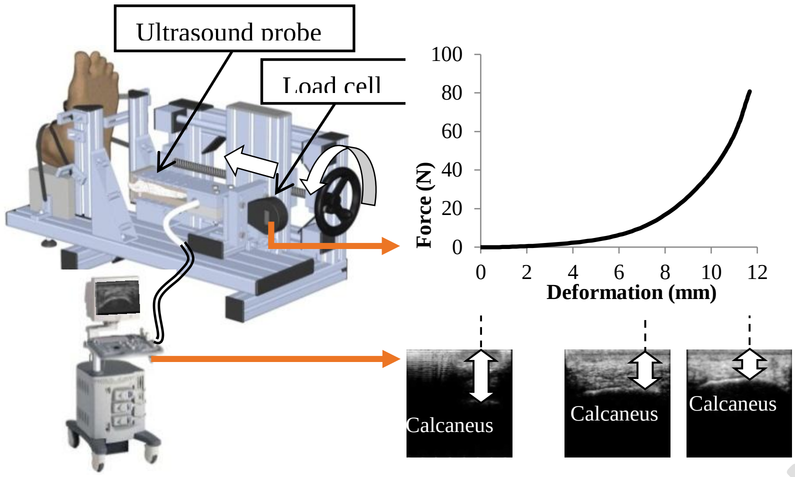
Ultrasound probe
Load cell
100
80
60
40
20
0
Force (N)
0
2
4
6
8
10
12
Deformation (mm)
Calcaneus
Calcaneus
Calcaneus

Figure 2

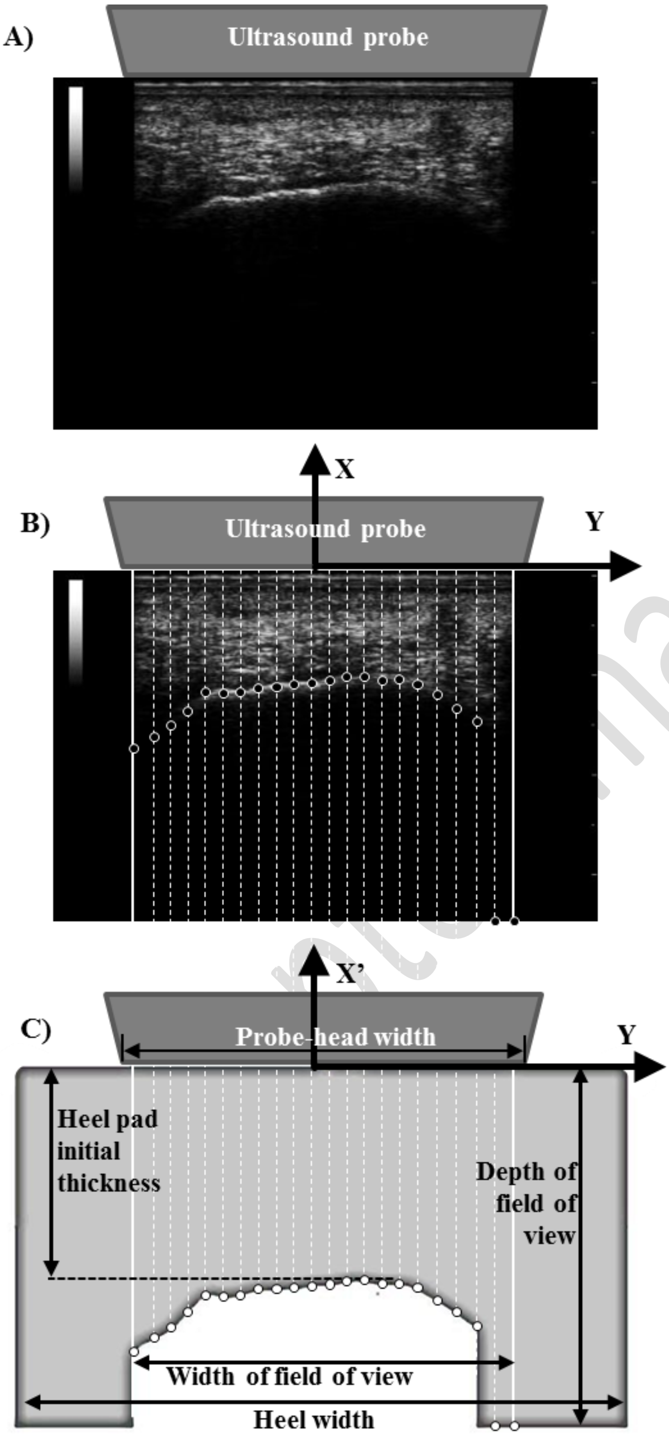
A)
Ultrasound probe
B)
Ultrasound probe
X
Y
C)
Probe-head width
X'
Y
Heel pad
initial
thickness
Depth of
field of
view
Width of field of view
Heel width

Figure 3

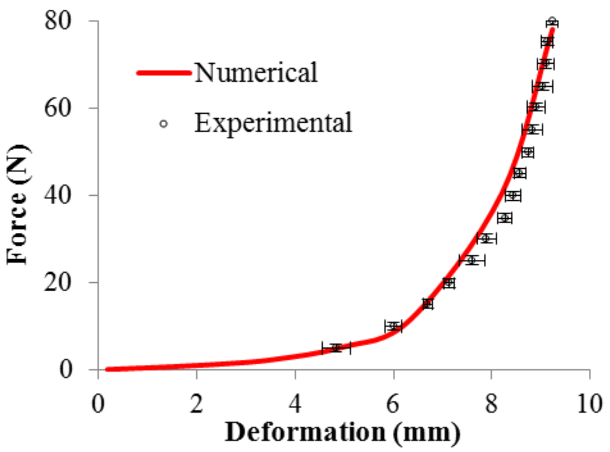

80
60
40
20
0
Force (N)
Numerical
Experimental
0
2
4
6
8
10
Deformation (mm)

Figure 4

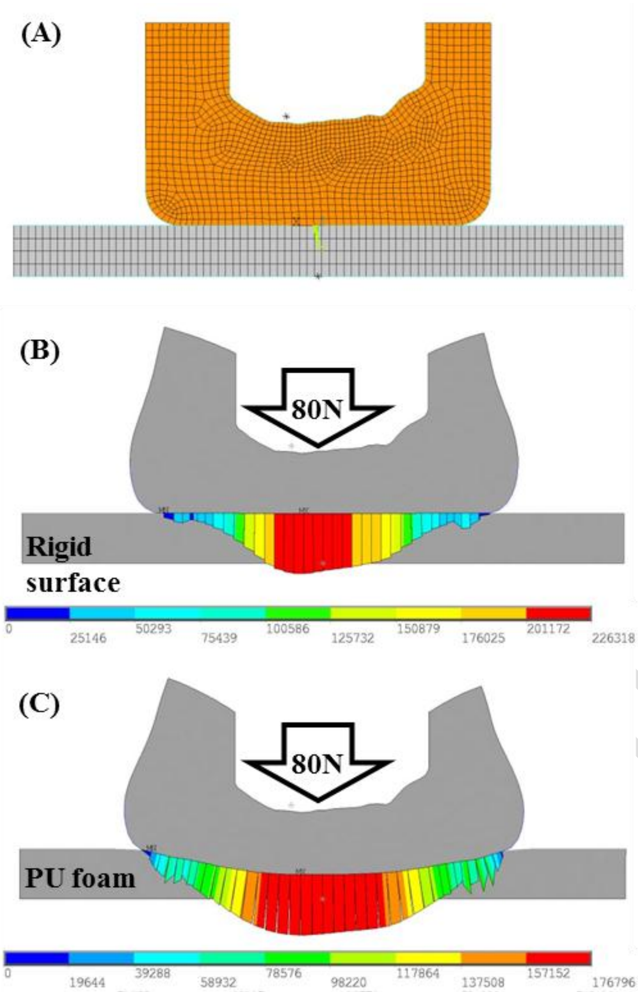
(A)
(B)
80N
Rigid
surface
0
25146
50293
75439
100586
125732
150879
176025
201172
226318
(C)
80N
PU foam
0
19644
39288
58932
78576
98220
117864
137508
157152
176796

Figure 5

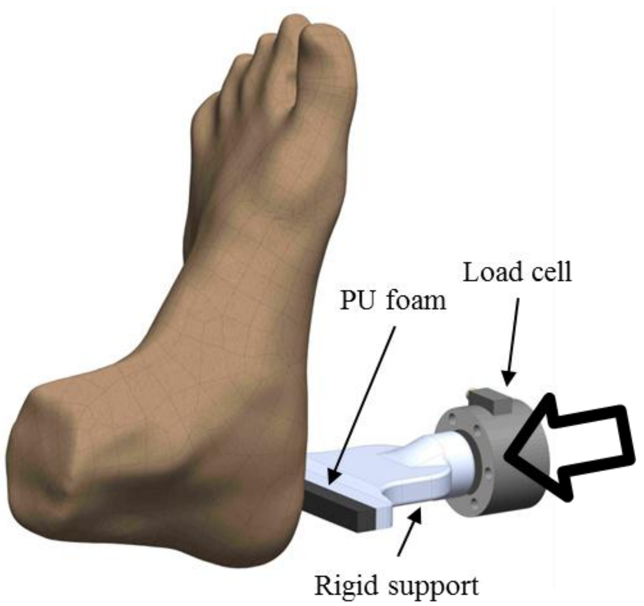

Figure 6

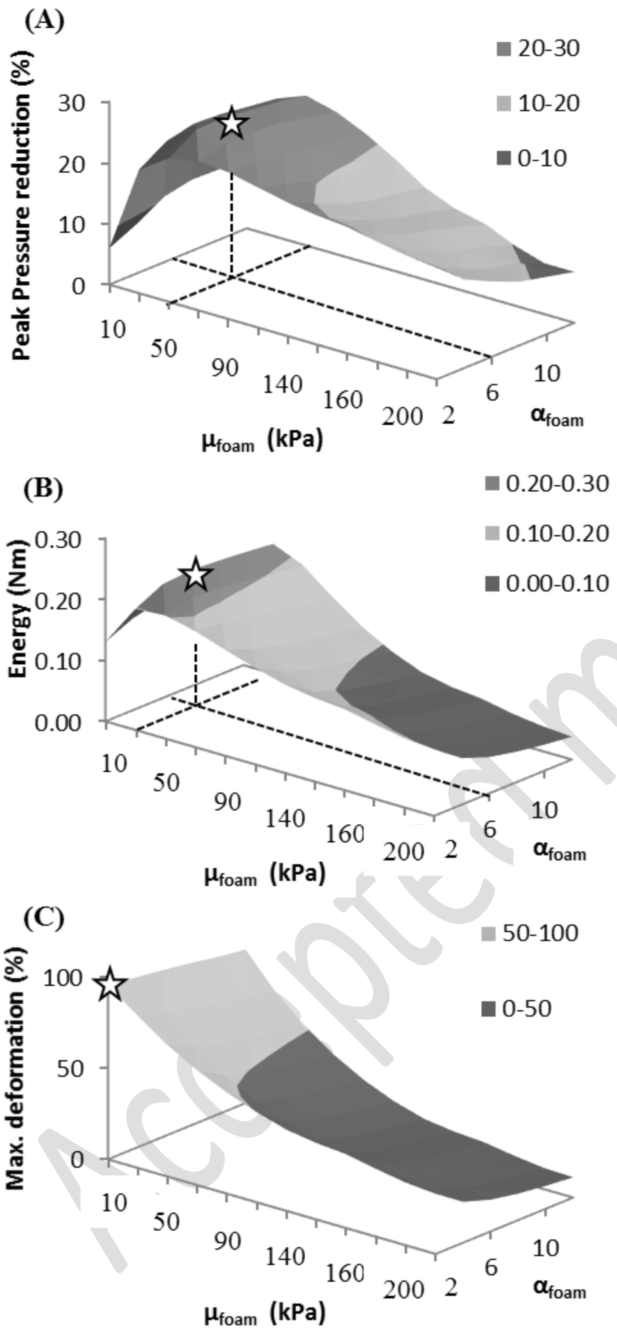
(A)
Peak Pressure reduction (%)
30
20
10
0
20-30
10-20
0-10
10
50
90
140
160
200
2
6
10
μ_{foam} (kPa)
α_{foam}
(B)
Energy (Nm)
0.30
0.20
0.10
0.00
0.20-0.30
0.10-0.20
0.00-0.10
10
50
90
140
160
200
2
6
10
μ_{foam} (kPa)
α_{foam}
(C)
Max. deformation (%)
100
50
0
50-100
0-50
10
50
90
140
160
200
2
6
10
μ_{foam} (kPa)
α_{foam}

Figure 7

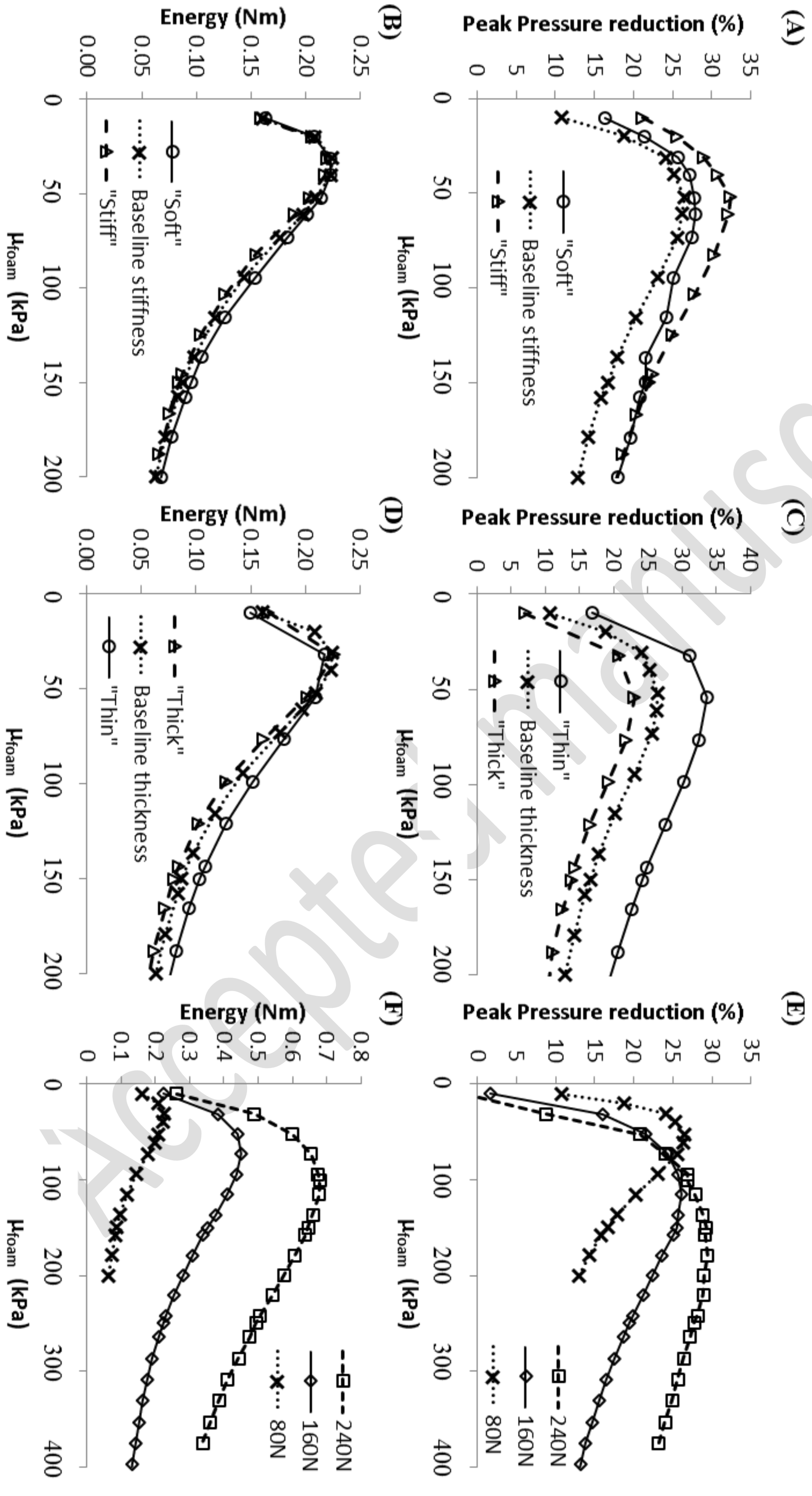

(A)
Peak Pressure reduction (%)
"Soft"
Baseline stiffness
"Stiff"
μfoam (kPa)
(B)
Energy (Nm)
"Soft"
Baseline stiffness
"Stiff"
μfoam (kPa)
(C)
Peak Pressure reduction (%)
"Thin"
Baseline thickness
"Thick"
μfoam (kPa)
(D)
Energy (Nm)
"Thick"
Baseline thickness
"Thin"
μfoam (kPa)
(E)
Peak Pressure reduction (%)
240N
160N
80N
μfoam (kPa)
(F)
Energy (Nm)
240N
160N
80N
μfoam (kPa)